Editors' Suggestion

Frequency measurement of the 2 $^1S_0$–3$^1D_2$ two-photon transition in atomic ^{4}He

Yi-Jan Huang,[1] Yu-Chan Guan,[1] Yao-Chin Huang,[2] Te-Hwei Suen,[2] Jin-Long Peng,[3] Li-Bang Wang,[2,*] and Jow-Tsong Shy[1,2,†]

[1]*Institute of Photonics Technologies, National Tsing Hua University, Hsinchu 30013, Taiwan*

[2]*Department of Physics, National Tsing Hua University, Hsinchu 30013, Taiwan*

[3]*Center for Measurement Standards, Industrial Technology Research Institute, Hsinchu 30011, Taiwan*

(Received 13 October 2017; published 26 March 2018)

We present precise frequency measurement of the 2 $^1S_0$-3 $^1D_2$ two-photon transition in ^{4}He at 1009 nm. The laser source at 1009 nm is stabilized on an optical frequency comb to perform the absolute frequency measurement. The absolute frequency of 2 $^1S_0$-3 $^1D_2$ transition is experimentally determined to be 594 414 291.803(13) MHz with a relative uncertainty of 1.6×10^{-11}, which is more precise than previous determinations by a factor of 25. In combination with the theoretical ionization energy of the 3 $^1D_2$ state, the ionization energy of the 2 $^1S_0$ state is determined to be 960 332 040.823(24) MHz. In addition, the deduced 2 $^1S_0$ and 2 $^3S_1$ Lamb shifts are 2806.864(24) MHz and 4058.130(24) MHz, respectively, which are 1.6 times better than previous determinations, and the fine structure 3 $^3D_1$-3 $^1D_2$ is determined to be 101 143.889(29) MHz, improving the precedent determination by a factor of 11.

DOI: 10.1103/PhysRevA.97.032516

I. INTRODUCTION

Helium is the simplest multielectron atom and it plays a crucial role in testing many-body quantum electrodynamics (QED) calculations. Recently, the electronic structure of helium has been calculated to a very high precision [1–5]. Theoretical calculations with terms in α^2 and α^4 describe the gross structure and the first relativistic corrections, respectively, where α is the fine-structure constant. The Lamb shift is included in the α^5, α^6, and α^7 terms. The theoretical uncertainty of the Lamb shift ranges from 0.5 to 2 MHz for the $n = 2$ states and is mainly due to the term in α^7 [5]. For the experimental verification of the Lamb shift, the two metastable states of helium, the low-lying triplet 2 $^3S_1$, and singlet 2 $^1S_0$ states have large QED effects and can be accessed by commercially available visible or IR laser sources and therefore are of great theoretical and experimental interest. In the experimental respect, to determine the Lamb shift of the $2S$ states, the measurements of the $2S$-nD two-photon transitions are typically chosen since the theoretical uncertainties of the D states are much smaller than the low-lying S and P states. For example, the Lamb shift of the 2 $^3S_1$ state has been determined using the 2 $^3S_1$-3 $^3D_1$ two-photon transition [6], and the Lamb shift of the 2 $^1S_0$ state has been determined using the 2 $^1S_0$ – n $^1D_2$ two-photon transitions ($7 < n < 20$) [7]. In addition, the highly precise frequency measurement of the 2 $^1S_0$-2 $^3S_1$ doubly forbidden transition [8] at 1557 nm serves as a bridge to connect the triplet and singlet states. For example, the Lamb shift of the 2 $^1S_0$ state can be determined from the 2 $^3S_1$-3 $^3D_1$ transition [6] and 2 $^3S_1$-2 $^1S_0$ transition [8]. Due to the recent developments of the optical frequency comb (OFC), several OFC-based measurements have been performed to directly determine the absolute transition frequencies of He [8–15]. The best previous determination of the Lamb shift of the 2 $^1S_0$ state in ^{4}He is 2806.803(35) MHz, obtained from precise measurements of the ^{4}He 2 $^3S_1$-2$^3P_0$ [9,10], 2 $^3P_0$-3 $^3D_1$ [15], and 2 $^3S_1$-2 $^1S_0$ transitions [8].

In this work, we present our precise absolute frequency measurement of the singlet 2 $^1S_0$-3 $^1D_2$ two-photon transition at 1009 nm. The uncertainty reaches 13 kHz, and we are able to reduce the uncertainty of the ionization energy of the 2 $^1S_0$ state and the Lamb shift of both the 2 $^1S_0$ and 2 $^3S_1$ states to an uncertainty of 24 kHz, which is limited mostly by the uncertainty of the theoretical ionization energy of the $3D$ states (20 kHz). In addition, combining with other precise ^{4}He measurements [8–10,15], we determine the separation between 3 $^3D_1$ and 3 $^1D_2$ with a 29-kHz uncertainty.

II. EXPERIMENTAL SETUP

The schematic of our experimental setup is shown in Fig. 1. The 1009-nm light source used for the 2 $^1S_0$-3 $^1D_2$ two-photon transition in ^{4}He is a homemade external-cavity diode laser (ECDL). The laser is prestabilized onto a Fabry-Pérot (FP) cavity by the Pound-Drever-Hall locking technique [16], and its laser linewidth is reduced to below 250 kHz at 1-ms integration time observed using the beat note between the ECDL output and one comb line of an OFC. The OFC is based on a femtosecond Er-doped fiber laser [17]. For our experiment, we amplify its output and extend its supercontinuum spectrum from 1050 nm to 980 nm by a high nonlinear fiber. Both its repetition rate (f_r, 250 MHz) and offset frequency (f_o) are locked to microwave synthesizers phase-locked to a cesium clock (Microsemi, 5071A). The accuracy of the OFC is better than 1×10^{-12} at an integration time of 100 s. The laser frequency is locked on one comb line of the OFC by the offset locking technique. To increase the optical power for the two-photon transition, the output power of the ECDL is boosted

*lbwang@phys.nthu.edu.tw
†shy@phys.nthu.edu.tw

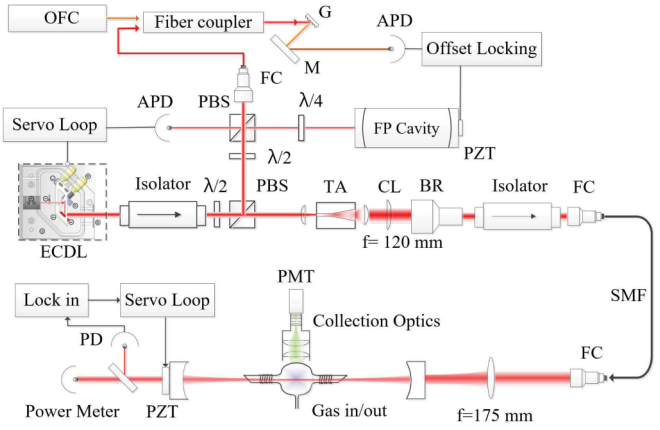

FIG. 1. The schematic diagram of the experimental setup for absolute frequency measurement of the $2\,^1S_0$-$3\,^1D_2$ two-photon transition in ^{4}He. The output of the 1009-nm external-cavity diode laser (ECDL) is divided into three beams. One is referenced to a fiber-based optical frequency comb (OFC) via a fiber link for absolute frequency measurement, one is used to prestabilize the ECDL frequency with a Fabry-Pérot (FP) cavity, and the remaining beam is injected into the tapered amplifier (TA) to boost the laser power. We employ cavity enhancement absorption for the two-photon spectroscopy with the He gas cell inside a cavity. The PMT monitors the 668-nm fluorescence signal from $3\,^1D_2$ to $2\,^1P_1$ through the collection optics.

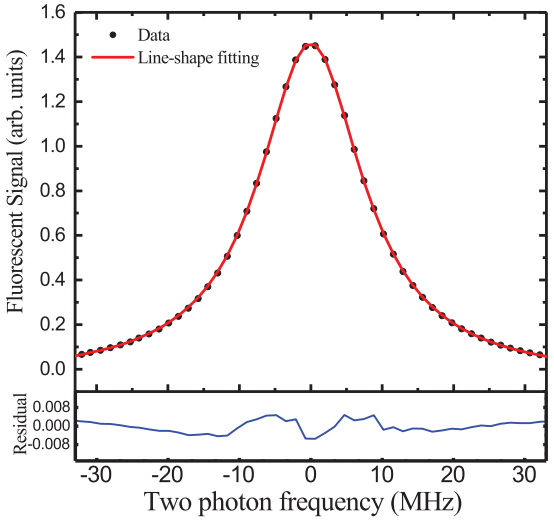

FIG. 2. A typical spectrum of the $2\,^1S_0$-$3\,^1D_2$ two-photon transition in ^{4}He. Here, optical power inside the power built-up cavity is 15 W, the pressure in the cell is 142.5 mTorr, and the rf discharge power is 3 W. A Lorentzian line shape (red line) is used to fit the observed spectrum.

to 2 W by a tapered amplifier (TA). After passing through an optical isolator and a single-mode optical fiber (SMF), we have a 750-mW laser beam with TEM_{00} profile for the two-photon spectroscopy.

Helium gas is filled in a glass cell and a radio-frequency (rf) discharge populates the $2\,^1S_0$ metastable state. The glass cell is a sphere (6 cm in diameter) sealed with Brewster windows at both ends. The spherical cell is helpful to avoid quenching of the metastable atoms due to collision on the wall. The glass cell is pumped by a turbomolecular pumping system to a pressure below 10^{-6} Torr, and its pressure can keep below 10^{-6} Torr with a getter (SAES CapaciTorr D 400-2) over one week after the cell is sealed. When the cell is filled with ^{4}He (typically 30–200 mTorr), the variation of the helium pressure is less than 1% over 2 weeks with rf discharge on. To enhance the optical power to excite the two-photon transition and also to obtain perfect overlapping counterpropagating laser beams, the cell is placed in a power built-up cavity formed by two spherical mirrors (200 mm radius of curvature, and 350 mm apart). The beam size of the waist is 156 μm. One mirror is mounted on a piezoelectric transducer (PZT) for cavity length tuning. To keep the cavity resonant with the laser frequency, the length of the cavity is locked on the transmission peak by dithering its PZT and the transmitted optical signal is demodulated using a lock-in amplifier. Then, to eliminate any possible Zeeman effect, the Earth magnetic field is shielded by a μ-metal box. The signal of the two-photon transition from monitoring the $3\,^1D_2$-$2\,^1P_1$ fluorescence at 668 nm is collected with an optical system consisting of two $f = 60$-mm lenses (3 inches in diameter), a near-infrared filter, an aperture of 1 inch in diameter, a 675-nm bandpass filter (30 nm FWHM), and a $f = 50$-mm lens in front of a photomultiplier tube (PMT). To avoid parasitic light, the rf discharge is pulsed at 10 kHz and the detection is carried out in the afterglow regime. At first, the rf power is switched on for a 5-μs duration, and then the PMT signal is collected for a 40-μs duration 20 μs after the rf is turned off. The laser frequency is scanned step by step with an interval of approximately 1.6 MHz by tuning the repetition rate of the OFC. During the measurements, the fluorescence signal and the beat frequency (f_b) between the ECDL and the OFC are recorded by a computer for 6 s for each frequency step. The corresponding absolute frequency of the ECDL is given by: $f = n \times f_r + f_o + f_b$, where n is the mode number of the OFC. The above timing sequence is also accurately controlled by the computer. In addition, the laser frequency is simultaneously monitored by a wavelength meter (HighFinesse WD30) with a resolution of 10 MHz to assist us in determining the OFC mode number n.

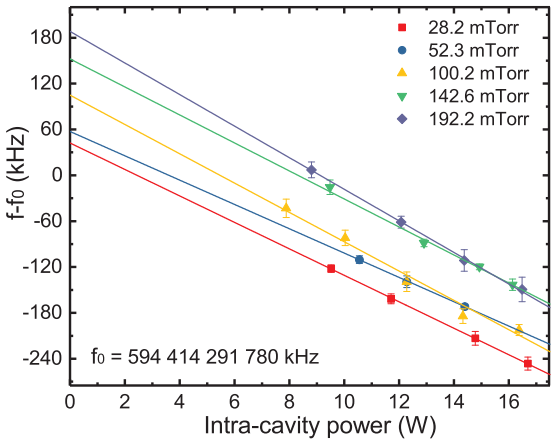

FIG. 3. The extrapolations of the transition frequency versus the intracavity optical power at five different pressures.

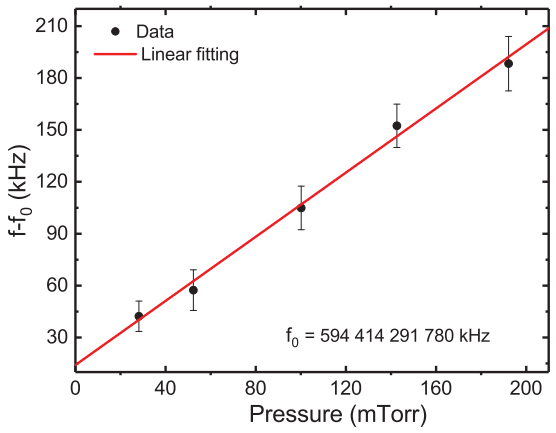

FIG. 4. The extrapolations of the frequency versus the pressure. Before correcting second-order Doppler shift, the 2 $^1S_0$-3 $^1D_2$ transition frequency at zero pressure and zero power is determined to be 594 414 291.796(13) MHz.

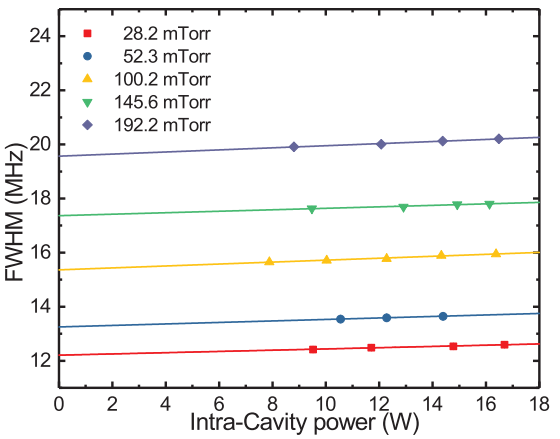

FIG. 5. The extrapolations of the FWHM versus intracavity power at five different pressures. The averaged power broadening coefficient is 23.1(2.6) kHz/W.

III. EXPERIMENTAL RESULTS

A typical spectrum of the 2 $^1S_0$-3 $^1D_2$ two-photon transition in ^{4}He is shown in Fig. 2. The locked laser frequency is scanned by tuning the repetition rate of the OFC. The spectrum has a linear background which is below 0.1% with respect to the signal. Since the ratio between the atomic lifetime of the 3 $^1D_2$ state and the transit time of the helium atom across the laser beam at the center of the power built-up cavity is 3 approximately, according to Ref. [18], we employ a Lorentzian line shape with a linear background to fit the spectrum, and the fitting achieves R^2 ε $>$ 99.99%. The fitting provides us the linewidth and the center frequency of the observed 2 $^1S_0$-3 $^1D_2$ transition.

We have measured the spectrum for five different pressures from 28 to 192 mTorr. For each pressure, the two-photon transition frequencies were measured with intracavity optical power from 8 to 16 W, as shown in Fig. 3. Each data point is obtained from 12 spectrums. The absolute pressure is measured by a MKS Baratron with an accuracy better than 1%, and its zero point is regularly checked at the pressure below 1×10^{-6} Torr. Furthermore, the intracavity power is determined by cavity-transmitting power, which is measured by a power meter (Thorlabs 302C) with an accuracy of 3%. Linear extrapolation to zero intracavity power allows us to correct the transition frequency shift caused by the ac-Stark shift. A constant fitting to the slopes of the transition frequency versus intracavity power is –18.6(9) kHz/W, which agrees with an estimate of the ac Stark shift taking the $n \leqslant 10$ singlet states into account. The intercepts of the linear extrapolations in Fig. 3 are the transition frequencies in different pressures at zero power, and then they are plotted versus pressure to determine the transition center frequency at zero power and zero pressure using the linear extrapolation shown in Fig. 4. The coefficient of transition frequency versus pressure is 927(92) kHz/Torr.

The effects of other experimental conditions are also investigated. The rf discharge does not have a significant effect on the transition frequency and spectral linewidth as we vary the rf power from 1 to 5 W. This can be understood since we take the data after the discharge is turned off. In addition, we measured the residual magnetic field inside the shielding μ-metal box and it is below 1 mG. Therefore, the evaluated Zeeman shift is below 1 kHz. Last, the second-order Doppler correction has been considered. By assuming the discharge temperature between 300 and 400 K, the correction is about 7.2(10) kHz. The experimental uncertainties are listed in Table I. Taking the frequency shifts and uncertainties into account, the frequency of the 2 $^1S_0$-3 $^1D_2$ transition in ^{4}He is determined to be 594 414 291.803(13) MHz. This result is in good agreement with a previous determination, 594 414 291.999(334) MHz, using the 2 $^1S_0$-2 $^1P_1$ [11,12] and the 2 $^1P_1$-3 $^1D_2$ transitions [13], and the precision is improved by a factor of 25.

TABLE I. Uncertainty of the 2 $^1S_0$-3 $^1D_2$ measurement.

Items	Uncertainty
Statistical uncertainty	12.8 kHz
Second-order Doppler effect	1 kHz
Zeeman effect	<1 kHz
OFC accuracy (multiple a factor of 2)	4 kHz
Overall uncertainty	13 kHz

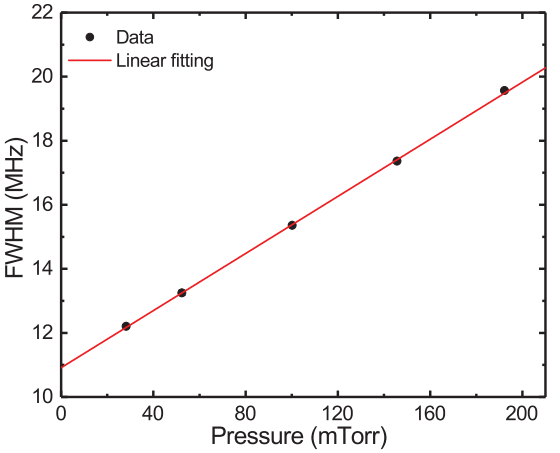

FIG. 6. The extrapolations of the FWHM at zero power versus the pressure. The FWHM at zero pressure and zero power is 11.21(7) MHz.

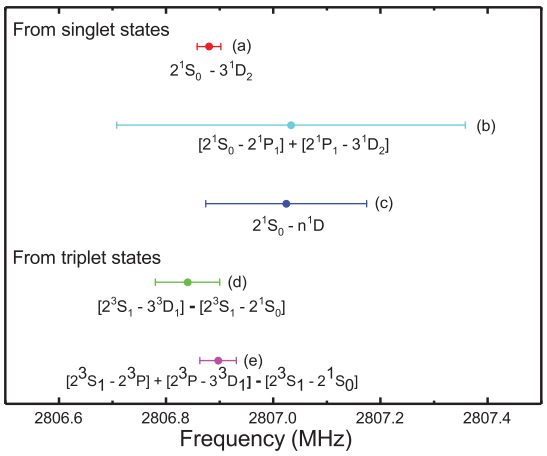

FIG. 7. The comparison of experimental determination of the $2\,^1S_0$ Lamb shift: (a) this work and (b) Refs. [11–13], (c) Ref. [7], (d) Refs. [6,8], and (e) Refs. [8–10,15].

We also investigate the power and pressure broadening effects to the linewidth of the two-photon transition. The power broadening linewidths for different pressures are shown in Fig. 5, and the averaged power broadening coefficient is 23.1(2.6) kHz/W. Then, the zero-power linewidth at different pressures are plotted in Fig. 6 to obtain the pressure broadening coefficient, 45.91(6) MHz/Torr. The linewidth of the two-photon transition at zero power and zero pressure, corresponding to the intercept of Fig. 6, is 10.91(7) MHz, which is in good agreement with the square root of the quadratic sum of the natural linewidth (10.36 MHz [19]) and the estimated transit time broadening linewidth (3.6 MHz) using the atomic velocity and the waist beam size in the power built-up cavity. The natural linewidth of the $2\,^1S_0$-$3\,^1D_2$ transition is mainly contributed from the lifetime of the $3\,^1D_2$ state (19.6 ms).

Combining the theoretical value of the $3\,^1D_2$ ionization energy 365 917 749.02(2) MHz from Ref. [1], we obtain the $2\,^1S_0$ ionization energy: 960 332 040.823(24) MHz. The contribution of the uncertainty is due to the theoretical calculation in the $3\,^1D_2$ state (20 kHz) and experimental uncertainty (13 kHz). The difference between our measurement and the theoretical value [960 332 038.0(1.7) MHz] is 2.8 MHz, which shows a discrepancy of 1.7σ. To deduce the Lamb shift on the $2\,^1S_0$ state, we subtract the nonrelativistic energy, the first relativistic corrections, and the finite nuclear size correction in Ref. [5] from our result. The $2\,^1S_0$ Lamb shift is deduced to be 2806.864(24) MHz. In Fig. 7, we compare our determination of the $2\,^1S_0$ Lamb shift with previous results by combining the theoretical values in $3D$ states and the triplet-state measurements using the $2\,^3S_1$-$2\,^1S_0$ measurement [8]. Our result is in good agreement with other determinations and is the most precise measurement at present, and it provides another independent test of the QED atomic theory. Furthermore, we make another comparison to avoid the large theoretical uncertainty of $2S$ states by using the more precise calculation of $3\,^1D_2$-$3\,^3D_1$ (28 kHz). We combine our result with precise measurements of the $2\,^3S_1$-$2\,^1S_0$ [8], $2\,^3S_1$-$2\,^3P_0$ [9,10], and $2\,^3P_0$-$3\,^3D_1$ [15] transitions to obtain the separation between $3\,^1D_2$ and $3\,^3D_1$ states, which has been of theoretical interest for the singlet-triplet mixing in $3D$ state. The result is in good agreement with theoretical calculation [1] and is listed in Table II. The uncertainty of the deduced separation of $3\,^1D_2$-$3\,^3D_1$ is 29 kHz, improving the precedent determination by a factor of 11, and the difference remains at 61 kHz. In addition, the Lamb shifts of the $2\,^1S_0$ and $2\,^1P_1$ states can be deduced more precisely by this work with previous measurements [11,12]. Our deduced Lamb shifts are listed in Table III along with the theoretical values.

TABLE II. Comparison of the $2\,^1S_0$-$3\,^1D_2$ and $3\,^3D_1$-$3\,^1D_2$ intervals with theory (unit: MHz).

	$2\,^1S_0$-$3\,^1D_2$	$3\,^3D_1$-$3\,^1D_2$
This work	594 414 291.803(13)	101 143.889(29)[a]
Theory	594 414 289.0(1.7)[b]	101 143.950(28)[c]
Difference	2.8	0.061

[a]In combination with Refs. [8–10,15].
[b]References [1,5].
[c]Reference [1].

TABLE III. The Lamb shifts of $2\,^1S_0$, $2\,^3S_1$, and $2\,^1P_1$ states (unit: MHz).

State	This work	Theory [5]
$2\,^1S_0$	2806.864(25)[a]	2809.7(1.7)
$2\,^3S_1$	4057.130(26) [b]	4058.6(1.3)
$2\,^1P_1$	47.39(18)[c]	48.87(40)

[a]In combination with Refs. [1,5].
[b]In combination with Refs. [1,5,8].
[c]In combination with Refs. [1,5,11,12].

IV. CONCLUSION

In conclusion, the absolute frequency of the $2\,^1S_0$-$3\,^1D_2$ two-photon transition of ^{4}He at 1009 nm is measured and a precision of 13 kHz is achieved. Our result is more precise than previous determinations using $2\,^1S_0$-$2\,^1P_1$ [11,12] and $2\,^1P_1$-$3\,^1D_2$ [13] transitions by a factor of 25. A new determination of the ionization energy of the $2\,^1S_0$ state is obtained using the theoretical ionization energy of the $3\,^1D_2$ state. It is consistent with the best previous determinations with 1.6 times improvement in precision. More importantly, we can deduce the most precise Lamb shift of the $2\,^1S_0$ state. In addition, the energy separation between the $3\,^3D_1$ and $3\,^1D_2$ states is deduced using the present result and other measurements and it agrees with theoretical calculation. In the near future, the absolute frequency measurement for $2\,^1S_0$-$3\,^1D_2$ two-photon transitions in ^{3}He will be performed to investigate the hyperfine structure of the $3\,^1D_2$ state in ^{3}He and the isotope shift between ^{3}He and ^{4}He. The long-standing discrepancy of the ^{3}He $3\,^3D_1$-$3\,^1D_2$ separation [1,20,21] will be resolved.

ACKNOWLEDGMENTS

We thank Chunghwa Telecom Laboratory for lending us a cesium clock. This project is supported by the Ministry of Science and Technology and the Ministry of Education of Taiwan. L.-B.W. acknowledges support from the Kenda Foundation as a Golden-Jade fellow.

[1] D. C. Morton, Q. Wu, and G. W. Drake, Can. J. Phys. **84**, 83 (2006).
[2] G. W. Drake and Z.-C. Yan, Can. J. Phys. **86**, 45 (2008).
[3] V. A. Yerokhin and K. Pachucki, Phys. Rev. A **81**, 022507 (2010).
[4] P.-P. Zhang, Z.-X. Zhong, Z.-C. Yan, and T.-Y. Shi, Chin. Phys. B **24**, 033101 (2015).
[5] K. Pachucki, V. Patkóš, and V. A. Yerokhin, Phys. Rev. A **95**, 062510 (2017).
[6] C. Dorrer, F. Nez, B. de Beauvoir, L. Julien, and F. Biraben, Phys. Rev. Lett. **78**, 3658 (1997).
[7] W. Lichten, D. Shiner, and Z.-X. Zhou, Phys. Rev. A **43**, 1663 (1991).
[8] R. Van Rooij, J. S. Borbely, J. Simonet, M. Hoogerland, K. Eikema, R. Rozendaal, and W. Vassen, Science **333**, 196 (2011).
[9] P. C. Pastor, G. Giusfredi, P. De Natale, G. Hagel, C. de Mauro, and M. Inguscio, Phys. Rev. Lett. **92**, 023001 (2004).
[10] P. C. Pastor, G. Giusfredi, P. De Natale, G. Hagel, C. de Mauro, and M. Inguscio, Phys. Rev. Lett. **97**, 139903 (2006).
[11] P.-L. Luo, J.-L. Peng, J.-T. Shy, and L.-B. Wang, Phys. Rev. Lett. **111**, 013002 (2013).
[12] P.-L. Luo, J.-L. Peng, J.-T. Shy, and L.-B. Wang, Phys. Rev. Lett. **111**, 179901 (2013).
[13] P.-L. Luo, Y.-C. Guan, J.-L. Peng, J.-T. Shy, and L.-B. Wang, Phys. Rev. A **88**, 054501 (2013).
[14] R. P. M. J. W. Notermans and W. Vassen, Phys. Rev. Lett. **112**, 253002 (2014).
[15] P.-L. Luo, J.-L. Peng, J. Hu, Y. Feng, L.-B. Wang, and J.-T. Shy, Phys. Rev. A **94**, 062507 (2016).
[16] R. Drever, J. L. Hall, F. Kowalski, J. Hough, G. Ford, A. Munley, and H. Ward, Appl. Phys. B **31**, 97 (1983).
[17] J.-L. Peng, H. Ahn, R.-H. Shu, H.-C. Chui, and J. Nicholson, Appl. Phys. B **86**, 49 (2007).
[18] F. Biraben, M. Bassini, and B. Cagnac, J. Phys. (Paris) **40**, 445 (1979).
[19] A. Wedding, A. Mikosza, and J. Williams, J. Electron. Spectrosc. Relat. Phenom. **52**, 689 (1990).
[20] J. Derouard, M. Lombardi, and R. Jost, J. Phys. (Paris) **41**, 819 (1980).
[21] F. S. Pavone, F. Marin, P. De Natale, M. Inguscio, and F. Biraben, Phys. Rev. Lett. **73**, 42 (1994).